Automated Computational Workflow for the Parametric Design and Optimization of a 3D-Printed Fin Ray Effect Soft Robotic Finger

Rodrigo Antunes[1,2][a], Luan Lang[1][b], Martim Lima de Aguiar[1,2][c], Nuno José Matos Pereira[1,2][d], Thiago Assis Dutra[1,2][e], Yebo Lu[3][f] and Pedro Dinis Gaspar[1,2][g]

[1]C-MAST, Centre for Mechanical and Aerospace Science and Technologies, University of Beira Interior, Calçada Fonte do Lameiro 6, 6200-358, Covilhã, Portugal

[2]Department of Electromechanical Engineering, University of Beira Interior, Calçada Fonte do Lameiro 6, 6200-358, Covilhã, Portugal

[3]College of Mechanical Engineering, Jiaxing University, Jiaxing, Zhejiang province, 314001, China

Keywords: Soft Robotic Finger, Computational Design, Fin Ray Effect, Parametric Optimization, Finite Element Analysis, Additive Manufacturing, PyAnsys, Soft Grippers.

Abstract: The design of soft grippers is challenged by the complex, non-linear coupling of material properties, geometry, and control, rendering traditional design methods inefficient. To address this, this paper presents an automated computational workflow for the parametric design and optimization of a 3D-printed Fin Ray Effect soft robotic gripper finger. The tool establishes a closed-loop digital thread, connecting a web-based parametric design interface using FreeCAD to a finite element analysis backend driven by PyAnsys. A parametric study was conducted, varying the number of internal crossbeams from 1 to 16, to analyse the gripper's performance using an experimentally validated hyperelastic model for TPU 60A. The results show a trade-off between contact pressure and pressure distribution, with an optimal configuration of 14-16 crossbeams identified for applications requiring a gentle grip with low-pressure concentrations. The developed workflow proved to be an effective method for rapidly iterating through designs and identifying an optimal solution, showcasing the power of automated simulation in the Design for Additive Manufacturing (DfAM) process.

1 INTRODUCTION

The field of robotics is evolving from a predominant emphasis on precision through rigidity toward an increasing integration of adaptability through compliance. For decades, rigid-linked robots have been the standard, however, they face considerable challenges when operating in unstructured, human-centric environments where safe interaction is required. Soft robotics presents an alternative, using materials such as elastomers and gels with moduli of elasticity, typically ranging from 10^4 to 10^9 Pa, which are comparable to biological tissues (Zhang et al., 2020). This material choice gives soft robotic grippers an inherent compliance (Nonaka et al., 2023), which enables them to passively adapt to objects of diverse and irregular shapes, absorb impact energy and reduce the need for complex control systems through a concept known as embodied intelligence (Ponce et al., 2021).

However, the very nature of these materials creates design challenges (Stella & Hughes, 2023), unlike in rigid robotics, the behaviour of a soft robot is governed by a tight, nonlinear coupling of its material properties, geometric morphology, and control inputs. This complexity renders traditional,

[a] https://orcid.org/0009-0002-6599-6905
[b] https://orcid.org/0000-0002-2857-3092
[c] https://orcid.org/0000-0003-0672-0378
[d] https://orcid.org/0000-0001-7177-751X
[e] https://orcid.org/0000-0002-3576-5703
[f] https://orcid.org/0000-0002-8995-370X
[g] https://orcid.org/0000-0003-1691-1709

Antunes, R., Lang, L., Lima de Aguiar, M., Pereira, N. J. M., Assis Dutra, T., Lu, Y. and Gaspar, P. D.
Automated Computational Workflow for the Parametric Design and Optimization of a 3D-Printed Fin Ray Effect Soft Robotic Finger.
DOI: 10.5220/0013944900003982

In *Proceedings of the 22nd International Conference on Informatics in Control, Automation and Robotics (ICINCO 2025) - Volume 2*, pages 577-584
ISBN: 978-989-758-770-2; ISSN: 2184-2809

intuition-based design methods inefficient and has created a need for advanced computational tools to navigate the design space effectively (Xie, Pinskier, et al., 2024).

To address this challenge, this paper presents an integrated computational workflow that automates the design and analysis of Fin Ray Effect (FRE) Soft Robotic Gripper Fingers (SRGF). The framework uses a web application to parametrically generate geometries in FreeCAD, which are then analysed using a Finite Element Method (FEM) simulation controlled programmatically via the PyAnsys library. The utility of this pipeline is demonstrated through a parametric study investigating the influence of internal crossbeam density on grasping forces and contact pressures, thereby contributing a practical tool for the principled design of high-performance soft robotic grippers.

2 LITERATURE REVIEW

2.1 Computational Approaches to Complex Design

Despite these conceptual advantages, the potential of soft grippers is constrained by the complexity inherent in their design (Stella & Hughes, 2023). Addressing these design complexities effectively requires moving beyond intuition-based approaches toward computational methods capable of navigating the high-dimensional and nonlinear design space of soft robotic grippers (Yi et al., 2025).

To overcome this, the field has increasingly embraced computational simulation as a tool for creating principled and optimized designs (Xie, Pinskier, et al., 2024). This approach formalizes the creative design process into an optimization task within a defined parameterized design space (Stella & Hughes, 2023). Researchers have focused on parameterizing key design variables, such as the spatial stiffness distribution for balancing compliance and force transmission, the geometry of pneumatic chambers for actuation (Navez et al., 2025), the finger arrangement and frame design, the selection and combination of materials to achieve controlled motion (Jin et al., 2024). The search for optimal parameters within this complex landscape has led to the widespread adoption of artificial intelligence techniques (Xie, Wang, et al., 2024). Methods such as Genetic Algorithms—which use a fitness function evaluated via simulation to evolve a population of designs —and Deep Reinforcement Learning have become mainstays in the field. A significant bottleneck, however, is the computational cost of fitness evaluation, which has been addressed by the use of Neural Network Surrogates to accelerate the process (Garcia et al., 2024).

Beyond parameter-based methods, more free-form approaches like topology optimization have been used to discover novel structures (Xie, Pinskier, et al., 2024). Furthermore, a holistic view recognizes that performance is determined by the synergy between morphology and control, leading to the goal of co-design—the simultaneous optimization of the robot's body and brain (Yi et al., 2025).

2.2 High-Fidelity Simulation with the Finite Element Method

At the core of any computational design framework resides the simulation engine, which predicts the physical behaviour of the gripper. The FEM allows for modelling hyperelastic body dynamics (Elgström, 2014), it is particularly well-suited for the challenges of soft robotics, which involve large, nonlinear material deformations. The process involves the discretization of the geometry into simpler elements and nodes, the reformulation of governing equations into a weak form, and the iterative solution of a large nonlinear system of equations, often using the Newton-Raphson method (Megan & Croop, 2014).

Modelling the hyperelastic behavior of elastomers was achieved using constitutive models such as the Neo-Hookean, Mooney-Rivlin, Yeoh and Polynomial models. An important step for simulation accuracy is the derivation of material coefficients by fitting these models to experimental test data, as these parameters are not typically found in datasheets (ANSYS Inc., 2017).

For gripper design, FEM allows for the simulation of contact mechanics—a challenging and non-smooth phenomenon. This includes enforcing non-penetration constraints, modelling friction, and analysing the resulting forces and pressure distributions during a grasp (Dassault Systèmes, 2018). For tasks that demand the highest degree of physical accuracy and validation, industry-standard commercial FEM packages like Ansys and ABAQUS are the preferred choice and are considered the gold standard for design verification (Han et al., 2020). The constant tension between simulation fidelity and computational speed remains a central engineering dilemma, driving the development of techniques like Reduced Order Modeling (Guo & Hesthaven, 2018) and learned surrogate models to manage this trade-off (Navez et al., 2025).

2.3 Integrated and Automated Workflows

The ultimate objective in computational design is the creation of fully automated pipelines that can autonomously discover, optimize, and validate novel designs. Recent breakthroughs in differentiable simulation and Quality Diversity (QD) algorithms are bringing this vision closer to reality (Xie, Wang, et al., 2024). Differentiable simulation allows for the use of highly efficient, gradient-based optimization algorithms (Connolly et al., 2015), while QD algorithms like MAP-Elites aim to generate a diverse archive of high-performing solutions rather than a single optimum (Xie, Pinskier, et al., 2024).

A technological enabler for automation is the development of Python libraries that provide programmatic access to powerful commercial solvers. The PyAnsys project, for example, is a collection of Python packages that enables users to set up, run, and post-process Ansys simulations entirely through scripts, bridging the gap between high-fidelity analysis and flexible automation (Maronehitz, 2024). These integrated, multi-physics workflows have been successfully applied to design complex structures. A powerful example is the framework developed for designing the GelSight Fin Ray, a compliant finger with embedded tactile sensing, which used a dual simulation pipeline to co-design its mechanical and sensory components (Liu et al., 2023; Liu & Adelson, 2022). This demonstrates both the viability of integrated simulation-driven design and the continued relevance of specific, high-performance structures like the FRE SRGF. Our work builds upon these advancements by presenting a specialized, integrated tool that leverages the power of PyAnsys to automate the design and detailed contact area and pressure analysis of FRE SRGF, addressing the practical need for accessible and efficient design-to-analysis pipelines for specific, high-performance structures within the broader landscape of soft robotics research.

2.4 Influence of Internal Number of Ribs in Fin Ray Effect Design Finger

An area of research within Fin Ray Effect finger design is the optimization of its internal structure, as the crossbeams (also known as ribs), are components that significantly influence the finger's overall stiffness and gripping performance. The number and angle of crossbeams have been identified as parameters impacting the balance between flexibility and force application (Shin et al., 2021; Suder et al., 2021). Shin et al., (2021) systematically investigated the effect of varying the number of crossbeams on finger performance, concluding that it had a significant impact on displacement. The analysis showed that as the number of crossbeams increased, the stress applied to a gripped object also increased, while the fingertip's displacement decreased due to the higher overall stiffness. This highlights a direct trade-off between gripping force and flexibility. Through their optimization process, the researchers determined that a configuration with five crossbeams provided the optimal balance, achieving the necessary displacement for a complete grip while maximizing force. Suder et al., (2021) also explored this relationship by testing fingers with 1 to 9 crossbeams. Using a deflection coefficient to mathematically evaluate the finger's ability to wrap around an object, the study found that the most suitable structure for wrapping was not the one with the highest deformation. While the finger with only one crossbeam deformed the most under a constant load, it did not achieve the best wrapping score. Instead, the analysis identified a structure with six crossbeams as having the best performance in terms of its wrapping capability. Table 1 summarizes the findings regarding the effect of the number of crossbeams in the Fin Ray finger design.

Table 1: Summary of Rib Number Influence in Fin Ray Effect Fingers Design.

Study	Shin et al., (2021)	Suder et al., (2021)
Crossbeams Investigated	Varied number, with a final design of 5	1 to 9 crossbeams
Finding on Stiffness & Deformation	Increasing the nº of crossbeams decreased finger displacement, resulting in a stiffer structure.	The finger with only 1 crossbeam showed the greatest deformation.
Finding on Force & Wrapping	Increasing the nº of crossbeams increased the stress applied to the object.	Wrapping ability was the primary metric; it did not directly correlate with maximum deformation.
Optimal Number & Rationale	5 crossbeams were found to be optimal for balancing the necessary displacement and force for a complete grip.	6 crossbeams provided the best wrapping capability, as determined by the lowest deflection coefficient.

3 MATERIALS AND METHODS

To facilitate the rapid design and optimization of a soft robotic gripper, a comprehensive computational tool was developed. This tool creates a closed-loop digital thread by integrating a web-based user interface for parametric geometry generation with a backend engine for automated finite element analysis (FEA) and data extraction.

3.1 Integrated Design and Simulation Pipeline

The tool is architected as a complete pipeline organized by a central Python script, which manages the user interface and coordinates the execution of specialized sub-processes for CAD generation and FEA simulation. The workflow (shown in Figure 2) begins with a user defining the gripper's geometric parameters via the web interface. These parameters are then passed to a Free CAD scripting engine that generates the required .step files for the components. Subsequently, the .step files are imported by a PyAnsys script, which automates the setup, solution, and post-processing within Ansys Mechanical. The final stage of the pipeline involves the script outputting the time-dependent performance data as CSV files, enabling quantitative comparison between design iterations.

3.2 Parametric Design Generation via Web Application

A web application built with the Gradio library serves as the front-end, allowing users to define the finger's design parameters (Table 2). These parameters are sent to a FreeCAD script that programmatically generates the 3D models of the finger, a target sphere, and a base connector, which are then exported as STEP files. For this study, a parametric analysis was performed by varying the number of crossbeams from 1 to 16, as this is a key parameter in the Fin Ray Effect design. All other geometric parameters, including the 50 mm sphere diameter, were held constant.

Table 2: Design parameters used by the developed computational tool to create the Fin Ray Effect Finger.

Parameter	Unit
Overall finger length	[mm]
Finger base width	[mm]
Finger depth	[mm]
Finger frame thickness	[mm]
Rear frame side amplitude	[mm]
Number of crossbeams	[-]
Beam thickness	[mm]
Minimum beam thickness	[mm]
Taper ratio	[-]
Crossbeam angle	[deg]

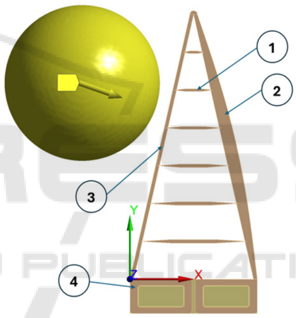

Figure 1: Architecture of the soft robotic finger and simulation setup. The finger consists of (1) Crossbeams, (2) a flexible rear spine, (3) the contact side, and (4) the finger base. A displacement is applied to the target sphere to simulate contact.

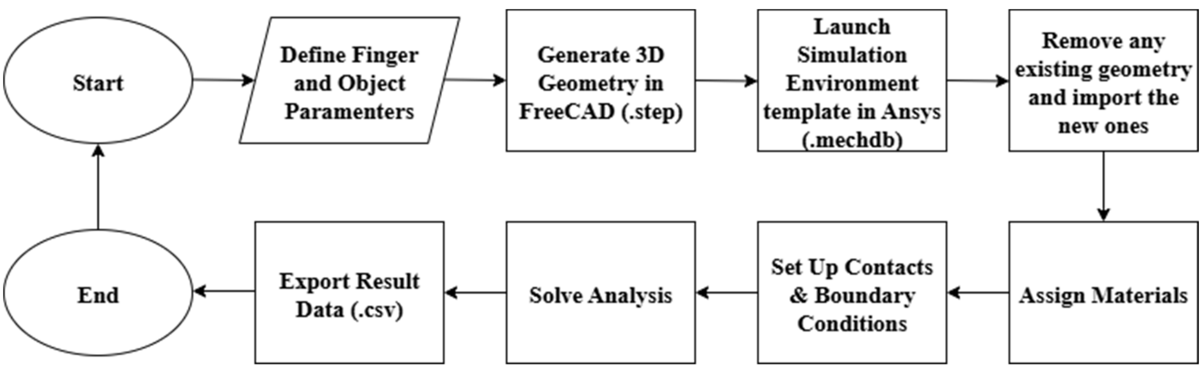

Figure 2: Flowchart of the automated computational workflow.

3.3 Automated Finite Element Analysis

The simulation is controlled by a PyAnsys script that automates the workflow in Ansys Mechanical. The script begins by opening a template project, replacing any existing geometry with the newly generated STEP files. Materials are then assigned programmatically, with a hyperelastic model for the TPU 60A finger and structural steel for the other components. The script automatically defines the necessary frictionless and bonded contacts and applies the boundary conditions for the linear actuation model. The analysis uses 10-node tetrahedral elements with contacts modelled using an Augmented Lagrange formulation.

3.4 Material Model Characterization

The mechanical behaviour of the flexible gripper material, TPU 60A, was determined through experimental testing in previous works (Lang et al., 2025). From this characterization, the stress-strain data was used as an input for the computational model. This experimental data was imported into Ansys Engineering Data, where the 2nd Order Polynomial hyperelastic model was selected for providing the best fit (R^2 = 0.9993), ensuring the simulated material behaviour reflects the real-world performance of the 3D-printed TPU 60A.

3.5 Simulation and Post-Processing

Once the model is generated, the script initiates the static structural analysis in Ansys Mechanical. To analyse the gripping performance, a Contact Tool is programmatically added to the solution and scoped specifically to the finger-object interface. After the solve is complete, the script automatically exports key results, such as the Force Reaction at the finger's base and the Contact Pressure distribution, to CSV files for quantitative analysis. This automated data extraction is critical for comparing the performance of different parametric designs.

4 RESULTS

The computational tool was employed to conduct a parametric study investigating the influence of the number of internal crossbeams on the performance of the FRE SRGF. A series of simulations was executed with 1, 2, 3, 4, 6, 8, 10, 12, 14, and 16 crossbeams, while all other geometric and simulation parameters were held constant, as defined in the materials and methods section. Four performance indicators—maximum contact pressure (P_{Max}), final reaction force (F_R), average contact pressure (P_{Avg})—were recorded at the final time step of each simulation to evaluate the gripper's design. A pressure uniformity ratio (U_P) was calculated according to Equation (1):

$$U_P = \frac{P_{Avg}}{P_{Max}} \tag{1}$$

This ratio serves as an indicator of grasping quality. In an ideal case, the contact pressure is evenly distributed, and the ratio approaches 1.

4.1 Effect on Maximum Contact Pressure

The relationship between the number of crossbeams and the resulting maximum contact pressure is shown in Figure 3. The trend is non-linear. The maximum pressure increases sharply from 0.03 MPa with one crossbeam to a peak of 0.20 MPa for designs with 6, 8, and 10 crossbeams. This initial rise corresponds to the increase in stiffness, which concentrates the gripping force onto smaller areas. Beyond 10 crossbeams, a clear downward trend is observed, with the maximum pressure decreasing to 0.15 MPa for the 16-crossbeam design.

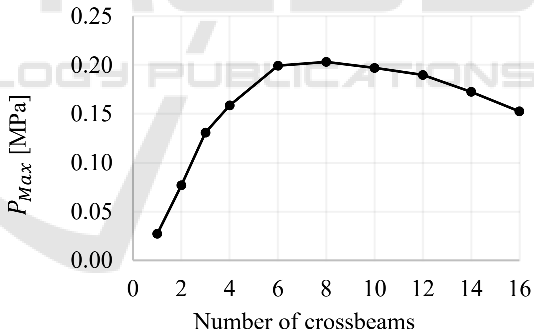

Figure 3: Maximum Contact Pressure applied in the last step of the simulation for each design configuration.

4.2 Effect on Gripping Force

The total reaction force indirectly indicates the overall gripping force exerted by the finger and is presented in Figure 4. The results show a clear and consistent trend as the number of crossbeams increases the reaction force steadily rises. The force increases from 0.85 N for a single crossbeam to a maximum of 1.67 N for the 16-crossbeam design. This indicates that adding more crossbeams progressively increases the structural stiffness of the finger, allowing it to generate a stronger grip for the same actuation displacement.

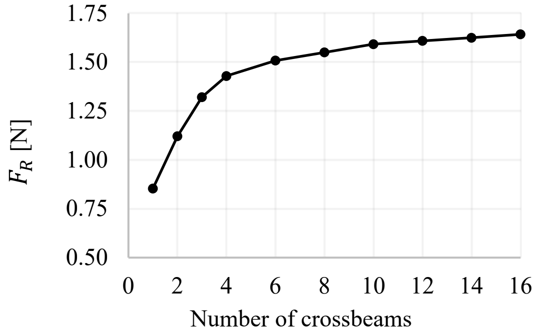

Figure 4: Force Reaction for each design configuration.

This condition together with the decrease of maximum pressure after 8 crossbeams demonstrates that a higher number of crossbeams distributes the load more effectively, reducing the intensity of pressure "hot spots."

4.3 Effect on Average Contact Pressure

The average contact pressure across the entire contact patch is presented in Figure 5. This metric shows a consistent upward trend, rising from 1.51 × 10^3 MPa for a single crossbeam to a peak of 3.13 × 10^3 MPa for the 14-crossbeam design. Unlike the maximum pressure, the average pressure does not decrease with a higher number of crossbeams, it is almost constant from the 10-crossbeam design to 16-crossbeam design. This suggests that while the peak pressures are reduced, the overall pressure across the contact area remains high and becomes more uniform, indicating a more efficient and distributed grip.

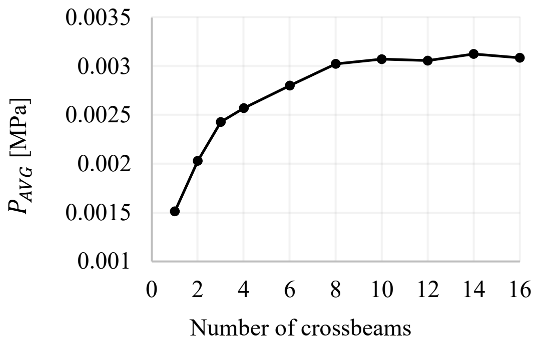

Figure 5: Average Contact Pressure applied in the last step of the simulation for each design configuration.

4.4 Effect on Pressure Distribution Uniformity

To quantify the uniformity of the grip, the ratio of the average pressure to the maximum pressure was calculated. A higher ratio signifies a more evenly distributed load. The results, plotted in Figure 6, show that the 1-crossbeam design had an exceptionally high uniformity ratio of 0.055, which is a consequence of its very low stiffness that results in low reaction force and max pressure. After this initial point, the uniformity drops significantly, reaching a minimum at 6 crossbeams where U_P = 0.014. As more crossbeams are added beyond this point, the pressure distribution becomes progressively more uniform, with the ratio steadily climbing to a new peak of U_P = 0.023 for the 16-crossbeam design. This trend suggests that a high number of crossbeams contributes to achieving an even and gentle grip.

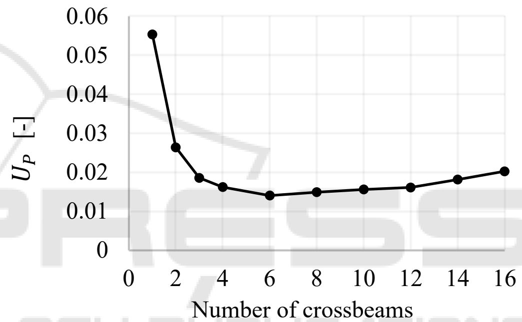

Figure 6: Ratio between Average Contact Pressure and Maximum Contact Pressure in each configuration as an evaluation parameter for pressure distribution.

4.5 Visual Analysis of Contact Pressure Maps

To visualize the qualitative trends underlying the quantitative data, Figure 7 displays the contact-pressure maps for four representative designs containing 2, 6, 10 and 14 cross-beams.

2 crossbeams (Figure 7a) – A narrow, vertically aligned band of increased contact pressure is observed. Local peaks occur where the lower crossbeam touches the object and at the fingertip, whereas a small zone in the top region shows lower contact pressure. The contact area is therefore large, but the finger is compliant and offers limited grasping stiffness, as indicated by the narrow contact region.

6 crossbeams (Figure 7b) – The pressure field becomes broader and lower. A zone of low pressure appears from mid-height to near the top, bounded by a second cross-beam footprint. A pronounced

pressure peak appears at the fingertip, indicating a configuration that may damage delicate objects.

As the number of crossbeams further increases to 10 (Figure. 7c) and 14 (Fig. 7d), the contact area continues to expand, and the load distribution becomes more uniform. Crucially, this reduces the maximum pressure at the fingertip, leading to a more stable and gentler grasp.

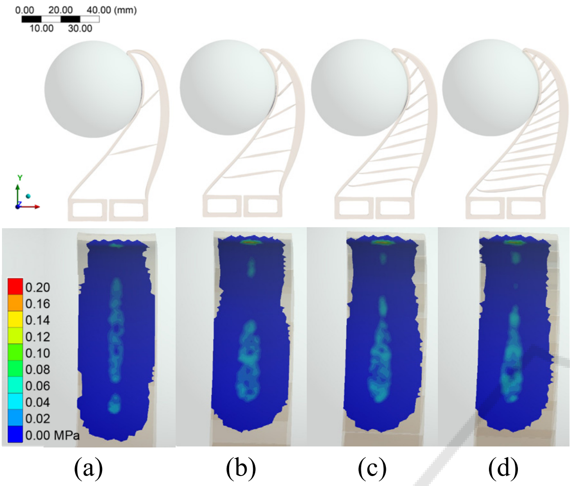

Figure 7: Finger Deformation and Contact Pressure Map at the end of the simulation for different number of crossbeams in the design, a) 2, b) 6, c) 10, d) 14.

Adding crossbeams initially raises the local peak pressure at the fingertip but further increases progressively equalise the pressure over the finger, reducing the peak value and improving grasp quality while maintaining adequate stiffness.

5 CONCLUSIONS

In this work, a comprehensive computational tool for the design and optimization of a 3D-printed, Fin Ray Effect robotic gripper was developed and validated. By integrating a parametric web interface with a FreeCAD geometry engine and a PyAnsys-driven finite element analysis backend, a closed-loop digital thread was created, enabling the rapid iteration and quantitative evaluation of different gripper designs.

The parametric study, which varied the number of internal crossbeams from 1 to 16 (1,2,3,4,6,8,10,12,14,16), revealed a complex and non-linear relationship between number of crossbeams and gripping performance. The results demonstrate that the relation between contact pressure, maximum pressure and grasping quality is not linear. Designs with 6 to 10 crossbeams exhibited a higher maximum contact pressure but at the cost of a poor pressure uniformity, characterized by a pressure peak near the fingertip. Conversely, designs with a high number of crossbeams (above 14) showed a marked improvement in performance in terms of pressure distribution. These configurations reduced the maximum contact pressure while simultaneously increasing the pressure distribution uniformity. The visual analysis of the contact pressure maps provided a qualitative confirmation of these findings, illustrating the transition from a focused, high-pressure grip to a more compliant and evenly distributed grip as the number of crossbeams was increased. Based on the simulation data, it can be concluded that for applications where minimizing pressure to a gripped object's surface is essential, a design with a higher number of crossbeams (e.g., 14-16) represents an optimal solution. This configuration provides a balance of a low maximum pressure, a bigger gripping force and a uniform pressure distribution.

Future work will investigate additional parameters influencing the performance of FRE SRGF, including crossbeam angles and material selection. Additionally, the fingertip design must be reevaluated to mitigate the maximum pressure hotspot and improve delicate object handling.

ACKNOWLEDGEMENTS

These results are within the research activities of project "ROBOTA-SUDOE - Robotics, Automation, and Digitalization as Drivers of Competitiveness and Growth for SMEs" (S1/1.1/P0125), which is co-funded by the European Union through the European Regional Development Fund (ERDF) and national funds, under the territorial cooperation Interreg Europe Programme 2021–2027 (eSUDOE 2021-2027). This research was partially funded by the Portuguese Foundation for Science and Technology, I.P. (FCT, I.P.) FCT/MCTES through national funds (PIDDAC), under the R&D Unit C-MAST/Center for Mechanical and Aerospace Science and Technologies, reference: Projects UIDB/00151/2020 (https://doi.org/10.54499/UIDB/00151/2020) and UIDP/00151/2020 (https://doi.org/10.54499/UIDP/00151/2020)

REFERENCES

ANSYS Inc. (2017). Appendix 4A: Hyperelasticity.

Connolly, F., Polygerinos, P., Walsh, C. J., & Bertoldi, K. (2015). Mechanical programming of soft actuators by varying fiber angle. Soft Robotics, 2(1), 26–32.

Dassault Systèmes. (2018). Modeling Rubber and Viscoelasticity with Abaqus.

Elgström, E. (2014). Practical implementation of hyperelastic material methods in FEA models.

Garcia, M., Esquen, A.-C., Sabbagh, M., Grace, D., Schneider, E., Ashuri, T., Voicu, R. C., Tekes, A., & Amiri Moghadam, A. A. (2024). Soft Robots: Computational Design, Fabrication, and Position Control of a Novel 3-DOF Soft Robot. Machines, 12(8), 539.

Guo, M., & Hesthaven, J. S. (2018). Reduced order modeling for nonlinear structural analysis using Gaussian process regression. Computer Methods in Applied Mechanics and Engineering, 341, 807–826. https://doi.org/10.1016/J.CMA.2018.07.017

Han, Y., Duan, J., & Wang, S. (2020). Benchmark problems of hyper-elasticity analysis in evaluation of FEM. Materials, 13(4), 885.

Jin, J., Feng, S., & Li, S. (2024). Computational Design of Customized Vacuum-Driven Soft Grippers. IEEE Robotics and Automation Letters.

Lang, L., Antunes, R., Dutra, T. A., Aguiar, M. L. de, Pereira, N., & Gaspar, P. D. (2025). Mechanical Characterization and Computational Analysis of TPU 60A: Integrating Experimental Testing and Simulation for Performance Optimization. Materials, 18(2). https://doi.org/10.3390/ma18020240

Liu, S. Q., & Adelson, E. H. (2022). GelSight Fin Ray: Incorporating Tactile Sensing into a Soft Compliant Robotic Gripper. http://arxiv.org/abs/2204.07146

Liu, S. Q., Ma, Y., & Adelson, E. H. (2023). GelSight Baby Fin Ray: A Compact, Compliant, Flexible Finger with High-Resolution Tactile Sensing. http://arxiv.org/abs/2303.14883

Maronehitz, P. (2024). Scripting for Mechanical Engineers.

Megan, L., & Croop, B. (2014). A Mechanism for the Validation of Hyperelastic Materials in ANSYS. Datapointlabs.

Navez, T., Ménager, E., Chaillou, P., Goury, O., Kruszewski, A., & Duriez, C. (2025). Modeling, Embedded Control and Design of Soft Robots using a Learned Condensed FEM Model. IEEE Transactions on Robotics.

Nonaka, T., Abdulali, A., Sirithunge, C., Gilday, K., & Iida, F. (2023). Soft robotic tactile perception of softer objects based on learning of spatiotemporal pressure patterns. 2023 IEEE International Conference on Soft Robotics, RoboSoft 2023. https://doi.org/10.1109/ROBOSOFT55895.2023.1012 1950

Ponce, H., Mart\'\inez-Villaseñor, L., & Mayorga-Acosta, C. (2021). Design of a soft gripper using genetic algorithms. Computación y Sistemas, 25(4), 835–842.

Shin, J. H., Park, J. G., Kim, D. Il, & Yoon, H. S. (2021). A Universal Soft Gripper with the Optimized Fin Ray Finger. International Journal of Precision Engineering and Manufacturing - Green Technology, 8(3), 889–899. https://doi.org/10.1007/s40684-021-00348-1

Stella, F., & Hughes, J. (2023). The science of soft robot design: A review of motivations, methods and enabling technologies. Frontiers in Robotics and AI, 9, 1059026.

Suder, J., Bobovský, Z., Mlotek, J., Vocetka, M., Oščádal, P., & Zeman, Z. (2021). Structural optimization method of a finray finger for the best wrapping of object. Applied Sciences (Switzerland), 11(9). https://doi.org/10.3390/app11093858

Xie, Y., Pinskier, J., Liow, L., Howard, D., & Iida, F. (2024). A'MAP'to find high-performing soft robot designs: Traversing complex design spaces using MAP-elites and Topology Optimization. 2024 IEEE/RSJ International Conference on Intelligent Robots and Systems (IROS), 11408–11415.

Xie, Y., Wang, X., Iida, F., & Howard, D. (2024). Fin-QD: A Computational Design Framework for Soft Grippers: Integrating MAP-Elites and High-fidelity FEM. 2024 IEEE 7th International Conference on Soft Robotics, RoboSoft 2024, 692–697. https://doi.org/10.1109/ROBOSOFT60065.2024.1052 1959.

Yi, S., Bai, X., Singh, A., Ye, J., Tolley, M. T., & Wang, X. (2025). Co-Design of Soft Gripper with Neural Physics. ArXiv Preprint ArXiv:2505.20404.

Zhang, C., Zhu, P., Lin, Y., Jiao, Z., & Zou, J. (2020). Modular soft robotics: Modular units, connection mechanisms, and applications. Advanced Intelligent Systems, 2(6), 1900166.